Electronic Supplementary Material (ESI) for Chemical Communications.

SUPPLEMENTARY INFORMATION

Tracking nitrite's deviation from Stokes-Einstein predictions with pulsed field gradient ^{15}N NMR spectroscopy

Trent R. Graham,[a]* Yihui Wei,[b] Eric Walter,[a] Emily T. Nienhuis,[a] Jaehun Chun,[a] Gregory K. Schenter,[a] Kevin M. Rosso,[a] Carolyn I. Pearce,[a,c] and Aurora E. Clark,[b]

(a) Pacific Northwest National Laboratory, Richland, Washington 99354, USA
(b) Department of Chemistry, University of Utah, Salt Lake City, Utah, 84112, USA
(c) Department of Crop and Soil Sciences, Washington State University, Pullman, Washington 99164, USA

(*) CORRESPONDING AUTHOR

Email: trent.graham@pnnl.gov

EXPERIMENTAL AND COMPUTATIONAL METHODOLOGY

S1. Sample preparation

The solutions of enriched $Na^{15}NO_2$ were prepared by the dissolution of sodium nitrite-^{15}N ($Na^{15}NO_2$, 98 atom % ^{15}N, Sigma Aldrich) in deionized water (18 MΩ·cm). Solutions of natural abundance $NaNO_2$ were prepared via dissolution of sodium nitrite (≥ 97.0 %, Sigma Aldrich) in deionized H_2O. Since the natural abundance of ^{15}N is approximately 0.37 %, the relative enrichment of the $Na^{15}NO_2$ samples is by a factor of approximately 265.

S2. NMR spectroscopy methodology

Proton nuclear magnetic resonance (NMR) spectroscopy was conducted on an 11.7467 T NMR spectrometer (Agilent/Varian) with a 5 mm broadband probe at 20°C. At 11.7467 T, the ^1H Larmor frequency is 500.130 MHz. The temperature of the sample was calibrated using the ^1H chemical shifts of ethylene glycol.[1] The single pulse, direct excitation ^1H NMR spectra were collected with a 4.99974 s acquisition time that was enumerated with 6677 complex points, a recycle delay of 1 s, a pulse width of 11.5 μs equivalent to a π/2 pulse width, a sweep width of 1335.5 Hz and with the collection of 1 transient. The ^1H chemical shifts are referenced to the resonance of ^1H_2O (18 MΩ·cm) where the resonance was assigned to 4.8 ppm. The ^1H NMR spectra were then processed in Mestrenova (version 14.0.1-22559, released 06/07/2019) where the spectra were zero-filled to 65536 points followed by 5 Hz of exponential line broadening. Additional spectra obtained with π/2 pulses were acquired for 1 m $Na_{15}NO_2$ at 20, 27, 40, 60, and 80 °C, and processed with 5 Hz of Lorenztian line broadening.

The ^1H PFGSTE-NMR spectra were collected on the same 11.7467 T NMR instrument with the DOSY gradient compensated stimulated echo with spin lock and convection compensation (DgcsteSL_cc) pulse sequence. The acquisition parameters include an acquisition time of 5 s enumerated with 6677 complex points, a sweep width of 1335.5 Hz, a recycle delay of 14 s, a π/2 pulse width of 11.5 μs, and 4 transients. The spatially dependent gradient pulses were arrayed linearly in 16 gradient steps, the durations of the spatially dependent gradient pulses were 1.1 ms, and the delay between gradient pulses was 50 ms. The pulse sequence incorporated 8 steady state pulses prior to the acquisition of data. The post-acquisition processing was performed in vNMRJ (v 4.2) where 5 Hz of exponential line broadening was applied. The diffusion coefficients were then calculated in vNMRJ using the modified spine model (SPLMOD) routine with a single component and the calculation utilized the integral of the resonance. The diffusion coefficients are referenced to the diffusion coefficient of ^1H_2O in water at an ethylene glycol calibrated temperature of 25°C.

Additional ^1H NMR experiments were acquired with an 11.7467 T NMR instrument on 1 m $Na^{15}NO_2$ at 20, 27, 40, 60, and 80 °C. For ^1H PFGSTE-NMR spectroscopy, the DGcsteSL_cc pulse sequence was again used with an acquisition time of 2.5 seconds enumerated by 6677 complex points and a recycle delay of 10 seconds. The sweep width was 2670.9 Hz. The diffusion delay

was 50 ms, 8 steady-state pulses were used, and 16 increments in gradient strength were acquired. For each increment in gradient strength, 16 transients were collected. For each temperature, the π/2 pulse length was calibrated, and the diffusion gradient length was optimized. The π/2 pulse lengths were approximately 12 μs and the optimized diffusion gradient length decreased from 1.3 ms to 0.9 ms at 20 and 80 °C, respectively. Post-acquisition processing was performed in vNMRJ where 5 Hz of exponential line broadening was applied. In vNMRJ, the SPLMOD routine was used to relate the attenuation of the integral to the diffusion coefficient of a single component. The diffusion coefficients are referenced to the diffusion coefficient of $^{1}H_2O$ in water at an ethylene glycol calibrated temperature of 25°C.

Single pulse, direct excitation ^{23}Na NMR spectroscopy was also performed on the 11.7467 T NMR spectrometer with the 5 mm broadband probe. The temperature of the sample was calibrated using the ^{1}H chemical shifts of ethylene glycol.[1] At 11.7467 T, the ^{23}Na Larmor frequency is 132.294 MHz. Parameters for the single pulse, direct excitation ^{23}Na NMR spectra include a 2.04416 s acquisition time enumerated with 1597 complex points, a recycle delay of 3 s, a pulse width of approximately 1.3 μs equivalent to a π/20 pulse width, a sweep width of 781.2 Hz and with the collection of 128 transients. The spectra are referenced to the ^{23}Na chemical shift of 1 M NaCl (Sigma-Aldrich, ≥ 99.0%) in H_2O, where the resonance was assigned to 0 ppm. The ^{23}Na NMR spectra were processed in Mestrenova. In Mestrenova, each ^{23}Na NMR spectrum was zero-filled to 4096 points and then 1 Hz of exponential line broadening was used. Additional spectra obtained with π/20 pulses were acquired for 1 m $Na_{15}NO_2$ at 20, 27, 40, 60, and 80 °C, and processed with 5 Hz of Lorenztian line broadening.

The ^{23}Na PFGSTE-NMR spectra were collected on the same 11.7467 T NMR spectrometer with the DgcsteSL_cc pulse sequence. Acquisition parameters include an acquisition time of 2.04416 s enumerated with 1597 complex points, a sweep width of 781.2 Hz, a recycle delay of 2.5 s, a π/2 pulse width of approximately 13 μs which was calibrated for each sample, and 64 transients. The spatially dependent gradient pulses were arrayed linearly in 16 gradient steps, the durations of the spatially dependent gradient pulses were 6.7 ms, and the delay between gradient pulses was 50 ms. The pulse sequence incorporated 16 steady-state pulses prior to the acquisition of data. Post-acquisition processing was performed in vNMRJ where 0.5 Hz of exponential line broadening was applied. The diffusion coefficients were also calculated in vNMRJ using the SPLMOD routine with a single component and the calculation utilized the integral of the resonance. The diffusion coefficients are referenced to the diffusion coefficient of $^{1}H_2O$ in water at an ethylene glycol calibrated temperature of 25°C.

Additional ^{23}Na NMR experiments were acquired with an 11.7467 T NMR instrument on 1 m $Na_{15}NO_2$ at 20, 27, 40, 60, and 80 °C. The DGcsteSL_cc pulse sequence was again used with an acquisition time of 2.0 seconds enumerated by 6388 complex points and a recycle delay of 1 second. The sweep width was 3125 Hz. The diffusion delay was 50 ms, 128 steady-state pulses were used, and 16 increments in gradient strength were acquired. For each increment in gradient strength, 128 transients were collected. For each temperature, the π/2 pulse length was calibrated, and the diffusion gradient length was optimized. The π/2 pulse lengths were approximately 12 μs

and the optimized diffusion gradient length decreased from 6.0 ms to 3.3 ms at 20 and 80 °C, respectively. Post-acquisition processing was performed in vNMRJ where 5 Hz of exponential line broadening was applied. In vNMRJ, the SPLMOD subprogram was used to relate the attenuation of the integral to the diffusion coefficient of a single component. The diffusion coefficients are referenced to the diffusion coefficient of $^{1}H_2O$ in water at an ethylene glycol calibrated temperature of 25°C.

Single pulse, direct excitation ^{15}N nuclear magnetic resonance (NMR) spectroscopy was performed on an 11.7467 T NMR spectrometer (Agilent/Varian) using a 5 mm broad band probe at 20°C. The temperature of the sample was calibrated using ^{1}H chemical shifts of ethylene glycol.[1] At 11.7467 T, the ^{15}N Larmor frequency is 50.697 MHz. Single pulse, direct excitation ^{15}N NMR spectra were collected with a 1.31072 s acquisition time enumerated with 131072 complex points, a recycle delay of 1 s, a pulse width of approximately 9.8 μs equivalent to a π/4 pulse width, a sweep width of 15060.2 Hz and with the collection of 4 transients. The spectra are referenced to the ^{15}N chemical shift of the 0.1 m $Na^{15}NO_2$ solution where the resonance was assigned to 0 ppm. The ^{15}N NMR spectra were processed in Mestrenova. In Mestrenova, each ^{15}N NMR spectrum was zero-filled to 262144 points and then 0.5 Hz of exponential line broadening was used. Additional spectra obtained with π/2 pulses were acquired for 1 m $Na_{15}NO_2$ at 20, 27, 40, 60 and 80 °C, and processed with 0.2 Hz of Lorenztian line broadening.

^{15}N PFGSTE-NMR spectra were collected on a 14.0954 T NMR spectrometer (Agilent/Varian) using a 5 mm PFG/Diffusion Liquids Z Gradient Probe (DOTY Scientific, pulsed gradient capability of 1380 G/cm) with the DgcsteSL_cc pulse sequence. Acquisition parameters include an acquisition time of approximately 2.51658 s enumerated with 512 complex points, a sweep width of 813.802 Hz, a recycle delay of 80 s, a π/2 pulse width of approximately 33.5 μs, and 256 transients (0.1 m $Na^{15}NO_2$ sample) or 16 transients (1, 6, and 12 m $Na^{15}NO_2$). The spatially dependent gradient pulses were arrayed linearly in 10 steps (0.1 m $Na^{15}NO_2$ sample) or 32 steps (1, 6, and 12 m $Na^{15}NO_2$), the durations of the spatially dependent gradient pulses were 1.7 ms, and the delay between gradient pulses was 50 ms. The pulse sequence incorporated 16 steady-state pulses prior to the acquisition of data. Post-acquisition processing was performed in vNMRJ where 2 Hz of exponential line broadening was applied. The diffusion coefficients were also calculated in vNMRJ using the SPLMOD routine with a single component and the calculation utilized the integral of the resonance. The diffusion coefficients are referenced to the diffusion coefficient of $^{1}H_2O$ in water at an ethylene glycol calibrated temperature of 25°C.

Additional ^{15}Na NMR experiments were acquired with a 11.7467 T NMR instrument on 1 m $Na_{15}NO_2$ at 20, 27, 40, 60 and 80 °C. The DgcsteSL_cc pulse sequence was again used with an acquisition time of 3.2 seconds enumerated by 4167 complex points and a recycle delay of 30 seconds. The sweep width was 1302.1 Hz. The diffusion delay was 400 ms, 64 steady-state pulses were used, and 16 increments in gradient strength were acquired. For each increment in gradient strength, 64 transients were collected. For each temperature, the π/2 pulse length was calibrated, and the diffusion gradient length was optimized. The π/2 pulse lengths were approximately 20 μs and the optimized diffusion gradient length decreased from 3.5 to 2.2 ms at 20 and 80 °C,

respectively. Post-acquisition processing was performed in vNMRJ where 0.2 Hz of exponential line broadening was applied. In vNMRJ, the SPLMOD subprogram was used to relate the attenuation of the integral to the diffusion coefficient of a single component. The diffusion coefficients are referenced to the diffusion coefficient of ^1H_2O in water at an ethylene glycol calibrated temperature of 25°C.

S3. Computational methodology

Classical Molecular Dynamics (CMD) simulations were performed for $NaNO_2$ aqueous solutions in GROMACS.[2] Molecule numbers and simulation box sizes are shown in Table 1. Each system was first equilibrated by a 5 ns NVT step at 300 K, followed by another 5 ns NPT step at 300 K. Production runs for diffusion coefficient data collection were then performed using 5 consecutive NVT steps at 300 K. Each one lasts for 5 ns with a fresh start to reduce drifting energy errors accumulated over the long simulations. Timesteps used in every simulation run are 1 fs. The Nove-Hoover thermostat[3, 4] and Parrinelo-Rahman barostat[5] were used for temperature and pressure coupling, respectively. A real-space cutoff of 0.9 nm was employed for the Van der Waals and short-range electrostatic interactions. The particle Mesh Ewald (PME) summation method[6] was employed to compute the long-range electrostatic energy. For the interatomic interactions, the SPC water model[7] and the $NaNO_2$ force field developed by Cordeiro et al.[8] were chosen. The parameters are listed in Table S2. LINCS algorithm[9] was used to constraint intramolecular O-H bonds in water molecules.

The diffusion coefficient D_A of particle type A is calculated using the following equation:

$$\lim_{t\to\infty}\langle\|\boldsymbol{r}_i(t)-\boldsymbol{r}_i(0)\|^2\rangle_{i\in A}=6D_At \qquad (1)$$

where $\boldsymbol{r}_i(t)$ is the position of atom i of particle type A at moment t and the left-hand side of the equation is the mean square displacement (MSD) of particle type A. The MSD from 1.1 m, 6 m and 13 m are shown in Figure S1. The error estimate is determined by linear regression of the MSD. The diffusion coefficients and errors shown in **Figure 2** in the main text are the average values of 5 independent simulations from production runs.

Table S1: Molecular compositions and simulation box volumes employed in the CMD simulations.

Concentration (m)	1.1	1.9	2.4	2.9	3.8
Number of $NaNO_2$ molecules	22	30	37	45	65
Number of H_2O molecules	1097	900	870	860	945
Volume (nm^3)	34.06	28.22	27.62	27.64	30.53

Concentration (m)	6	7	9.3	10.5	13
Number of $NaNO_2$ molecules	87	100	120	120	153
Number of H_2O molecules	805	790	720	633	655
Volume (nm^3)	27.34	27.74	26.81	24.11	26.78

Table S2: Force field parameters for $NaNO_{2(aq)}$ employed in this study.

Particle type	σ (nm)	ε (kJ/mol)	Charge (e)
Na	0.258	0.062	1
Ow	0.317	0.65	-0.82
Hw	0	0	0.41
N	0.334	0.438	0.4
O_N	0.263	1.725	-0.7

By analyzing an Na-centered coordinating polyhedron composed of a centroid Na ion, and several coordinating oxygen atoms (from either water or NO_2^-) as vertices, two dimensional histograms of ion-pair compositions can be determined using the PageRank algorithm.[10] When two polyhedrons share at least one oxygen vertices, they are connected and form an ion cluster of a dimer. A NO_2^- ion is part of a cluster if any of its two oxygens forms a vertex in the cluster.

The distributions of Na^+ and NO_2^- in ion species, such as free ions, single or multiple ion pairs (without forming a cluster), or complex ion clusters, are calculated as the percentage observation probability ($C_{i,j}$) in the entire simulation trajectory. The number of sodium in the ion species is denoted by variable i.The number of nitrite in the ion species is denoted by variable j.

The relative percent abundance ($X_{i,j}$) of an ion species comprised of i sodium and j nitrite is determined with Equation 2,

$$X_{i,j} = 100 \cdot \frac{(i+j)}{C_T} C_{i,j} \tag{2}$$

where C_T is the total number of ions in solutions.

$$C_T = \sum_{j=0}^{n} \sum_{i=0}^{n} (i+j) C_{i,j} \tag{3}$$

The pair-wise Radial Distribution Function (RDF) for atom pair ij is calculated using the following equation:

$$g_{ij}(r) = \frac{n_{ij}(r)}{4\pi r^2 dr \rho_j} \tag{4}$$

where $n_{ij}(r)$ is the number of atom j between distance r and $r + dr$ away from the reference atom i and ρ_j is the bulk density for particle j.

S4. Stokes-Einstein equation

The application of Stokes Einstein equation to pulsed field gradient NMR spectroscopy was reviewed elsewhere,[11] with a refinement regarding the application of indefinite association models.[12] For an infinitely dilute solute, the diffusion coefficient can be related to the hydrodynamic radius.

$$D = \frac{k_b T}{cf\pi\eta R_H} \tag{5}$$

where D is the mass averaged diffusion coefficient, k_b is the Boltzmann constant, T is the temperature, c is a friction coefficient, and η is the viscosity of the mixture, and R_H the hydrodynamic radius. For an infinitely dilute sodium nitrite dissolved in water comprised purely of free ions, the Boltzmann constant, temperature, and viscosity are the same for nitrite and sodium. Therefore, if also assuming the ions both exhibit slip or both exhibit non slip friction coefficients, the ratio of diffusion coefficients is related.

$$\frac{D_{NO2}}{D_{Na}} = \frac{R_{Na}}{R_{NO2}} \tag{6}$$

S5. Stejskal–Tanner equation

The Stejskal–Tanner relationship for a stimulated echo NMR pulse sequences is reviewed elsewhere.[12]

$$S(t + 2\tau) = \frac{M_0}{2} \cdot exp\left[\left(-\frac{2\tau}{T_2}\right) - \left(\frac{t}{T_1}\right)\right] \cdot exp\left[-D(\gamma g \delta)^2 \left(\Delta - \frac{\delta}{3}\right)\right] \tag{7}$$

In Equation 7, S is the amplitude of the stimulated echo, t is the storage period in which magnetization is in the z-plane, 2τ is the storage period in which magnetization is in the x- and y-plane, M_0 is the equilibrium magnetization, T_2 is the transverse relaxation coefficient, Δ is the duration between the onset of gradient pulses, γ is the gyromagnetic ratio of the nucleus, and g is the z-gradient magnitude.

S6. Vogel–Fulcher–Tammann (VTF) equation

The Vogel–Fulcher–Tammann (VTF) equation is a modification of the Arrhenius law,[13]

$$D(T) = D_v \cdot \exp\left(\frac{-E_a}{R(T - T_v)}\right) \tag{8}$$

where D is the temperature dependent diffusion coefficient, D_v is a pre-exponential factor, E_a is the activation energy associated with spatial translocation (diffusion), R is the universal gas constant (8.314×10^{-3} kJ K^{-1} mol^{-1}), T is temperature, and T_v is a fitting parameter.

Table S3. Data and VTF model fit for 1 m $Na^{15}NO_2$

Nucleus	Temperature [K]	Diffusion Coefficient [10^{-10} m^2 s^{-1}]	Standard Deviation [10^{-10} m^2s^{-1}]	VTF Prediction [10^{-10} m^2s^{-1}]	R^2
^{1}H	293.15	19.01	0.06	19.17	0.03
^{1}H	300.15	22.33	0.10	22.48	0.02
^{1}H	313.15	29.59	0.08	29.42	0.03
^{1}H	333.15	42.25	0.10	42.00	0.06
^{1}H	353.15	56.60	0.21	56.75	0.02
^{15}N	293.15	14.10	0.44	14.90	0.64
^{15}N	300.15	17.33	0.47	17.32	0.00
^{15}N	313.15	22.93	0.55	22.33	0.37
^{15}N	333.15	31.93	1.14	31.34	0.36
^{15}N	353.15	41.30	2.01	41.80	0.25
^{23}Na	293.15	10.85	0.30	10.88	0.00
^{23}Na	300.15	12.79	0.13	12.85	0.00
^{23}Na	313.15	17.12	0.11	17.00	0.02
^{23}Na	333.15	24.54	0.15	24.59	0.00
^{23}Na	353.15	33.55	0.40	33.54	0.00

Table S4. VTF model fit parameters for 1 m $Na^{15}NO_2$

	^{1}H	^{23}Na	^{15}N
E_a [kJ mol^{-1}]	7.68	7.91	7.52
D_v [10^{-10} m^2 s^{-1}]	2037.94	1470.94	1221.39
T_v [K]	95.17	86.01	101.55

ADDITIONAL RESULTS AND ANALYSES

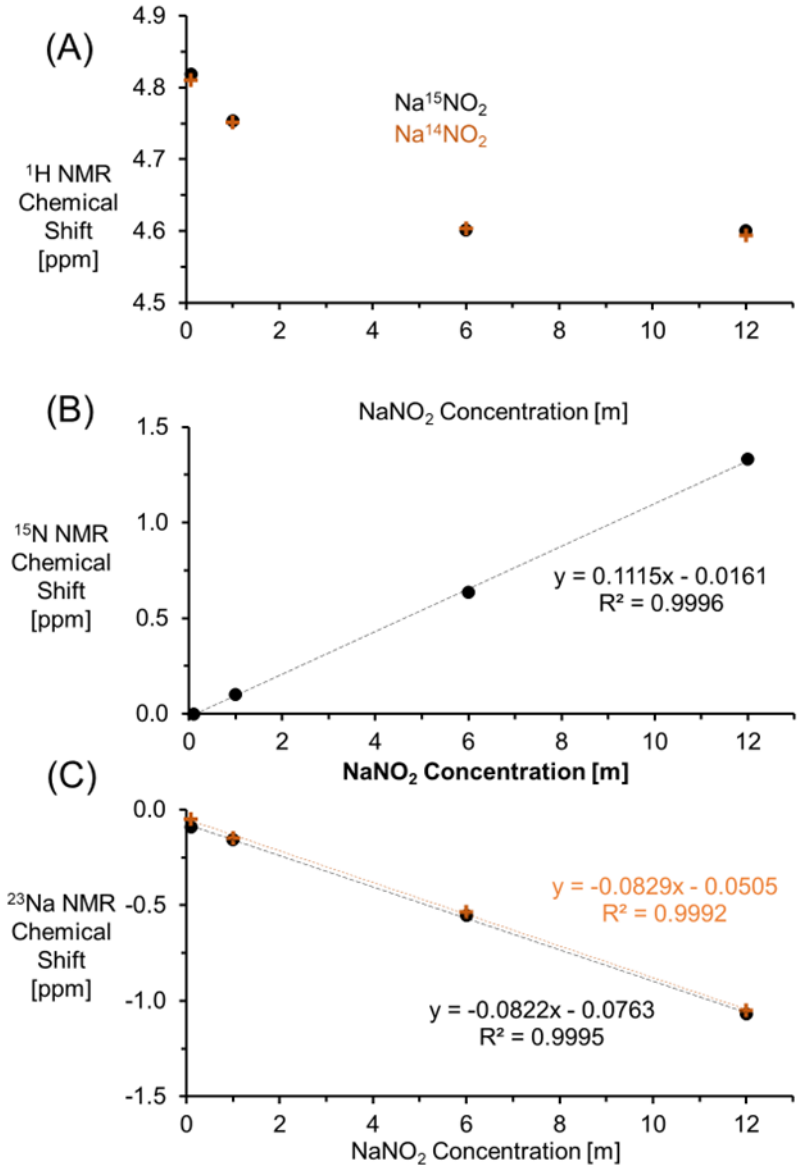

Figure S1. NMR chemical shifts of the (A) ^{1}H (B) ^{15}N and (C) ^{23}Na NMR resonances, demonstrating the near equivalence of the NMR chemical shifts in Na^{14}NO$_2$ and Na^{15}NO$_2$ solutions. Note that while the dependence of the chemical shift of the ^{15}N and ^{23}Na resonances are linear with respect to concentration, the chemical shift of ^{1}H exhibits nonlinear concentration dependence.

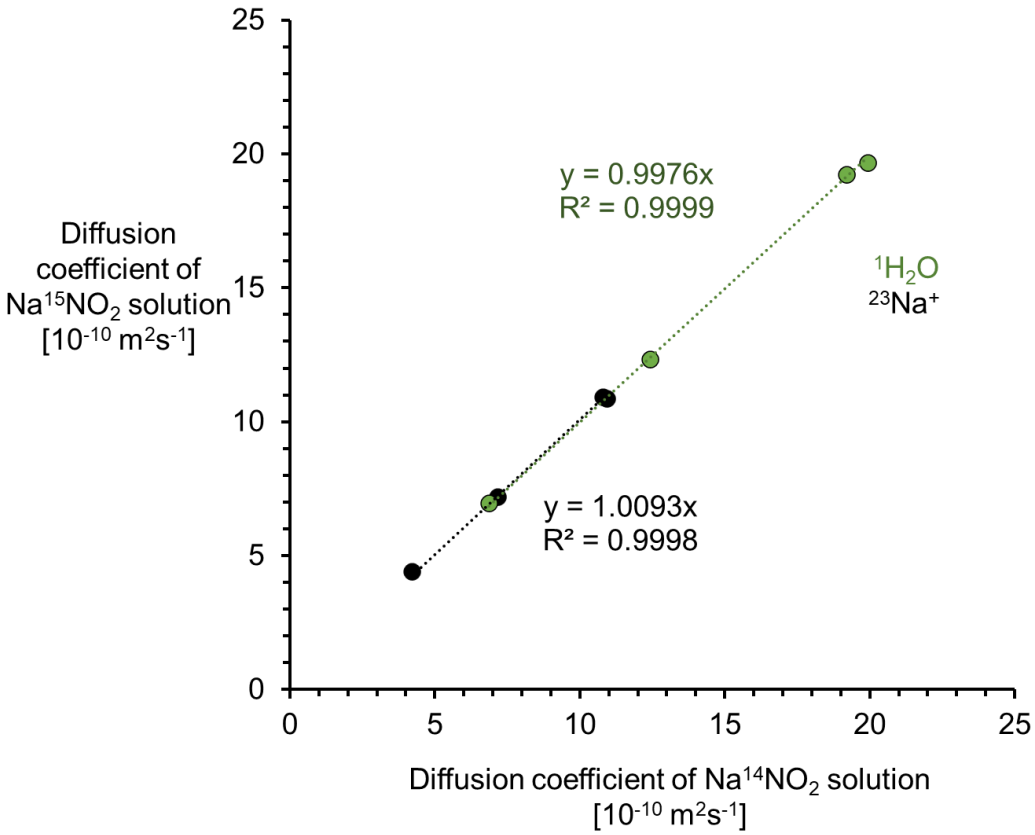

Figure S2. The correlation between the ^{1}H and ^{23}Na PFGSTE-NMR diffusion coeffients of the $Na^{14}NO_2$ and the $Na^{15}NO_2$ solution. The slope and R^2 are approximately 1 for both datasets, indicating that there are only trivial differences between the diffusion coefficients with respect to the isotope enrichment of $^{15}NO_2$.

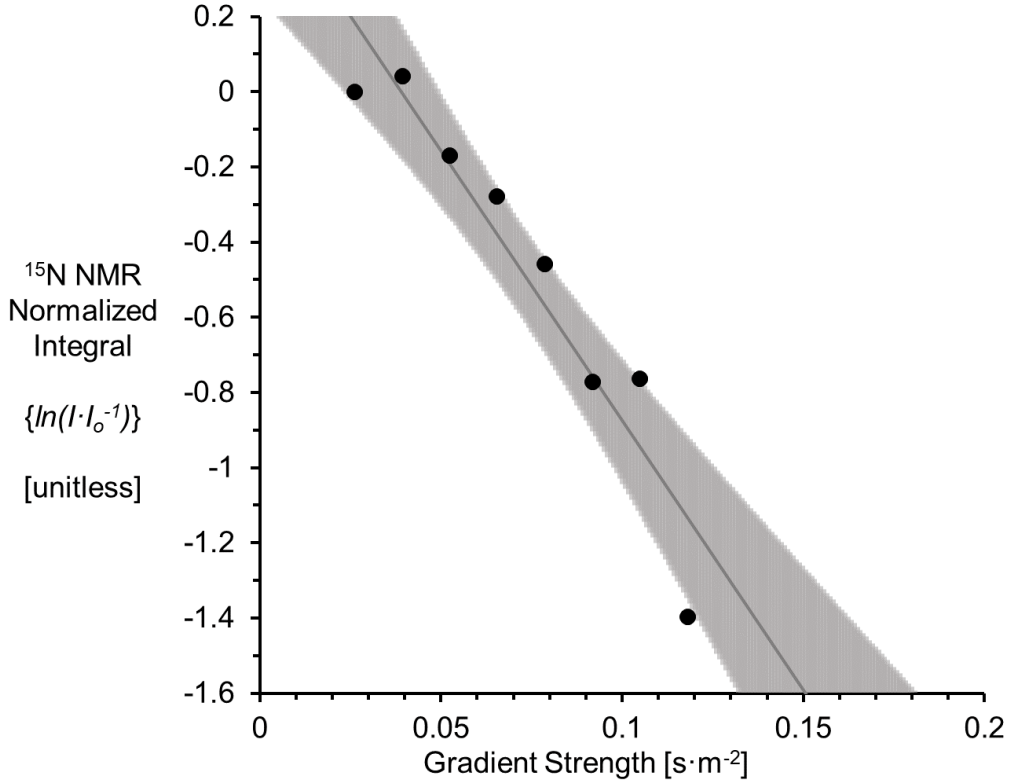

Figure S3. Stejskal-Tanner plot of the ^{15}N PFGSTE-NMR spectra of the 0.1 m $NaN^{15}NO_2$ sample at 20 °C.

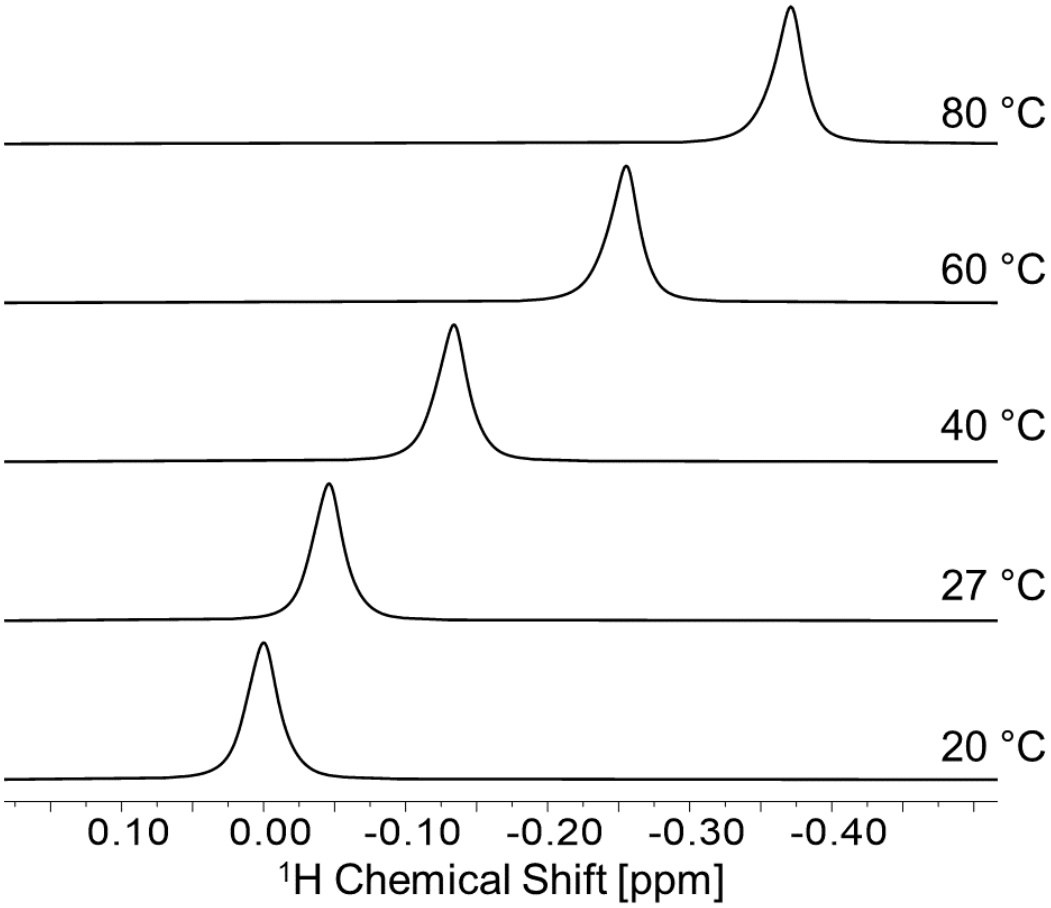

Figure S4. Single pulse, direct excitation ^{1}H NMR spectra of 1 m $Na^{15}NO_2$ at temperatures ranging from 20 to 80 °C. At all temperatures, a single resonance is observed, which is attributable to a distribution of water molecules in dynamic equilibrium that is fast relative to the NMR time scale. The spectra are normalized to the height of the resonance at each temperature. The chemical shift is referenced to the chemical shift of 1 m $Na^{15}NO_2$ at 20 °C.

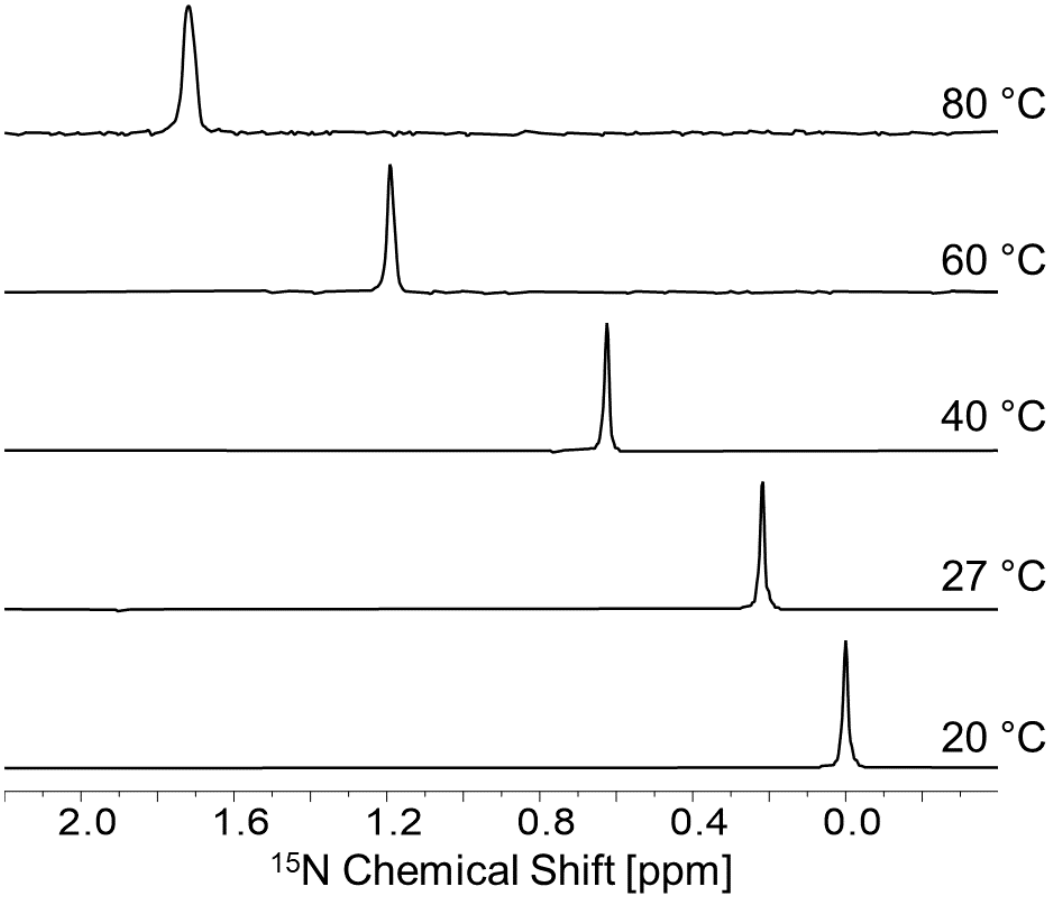

Figure S5. Single pulse, direct excitation ^{15}N NMR spectra of 1 m $Na^{15}NO_2$ at temperatures ranging from 20 to 80 °C. At all temperatures, a single resonance is observed, which is attributable to a distribution of NO_2^- ions in dynamic equilibrium that is fast relative to the NMR time scale. The spectra are normalized to the height of the resonance at each temperature. The chemical shift is referenced to the chemical shift of 1 m $Na^{15}NO_2$ at 20 °C.

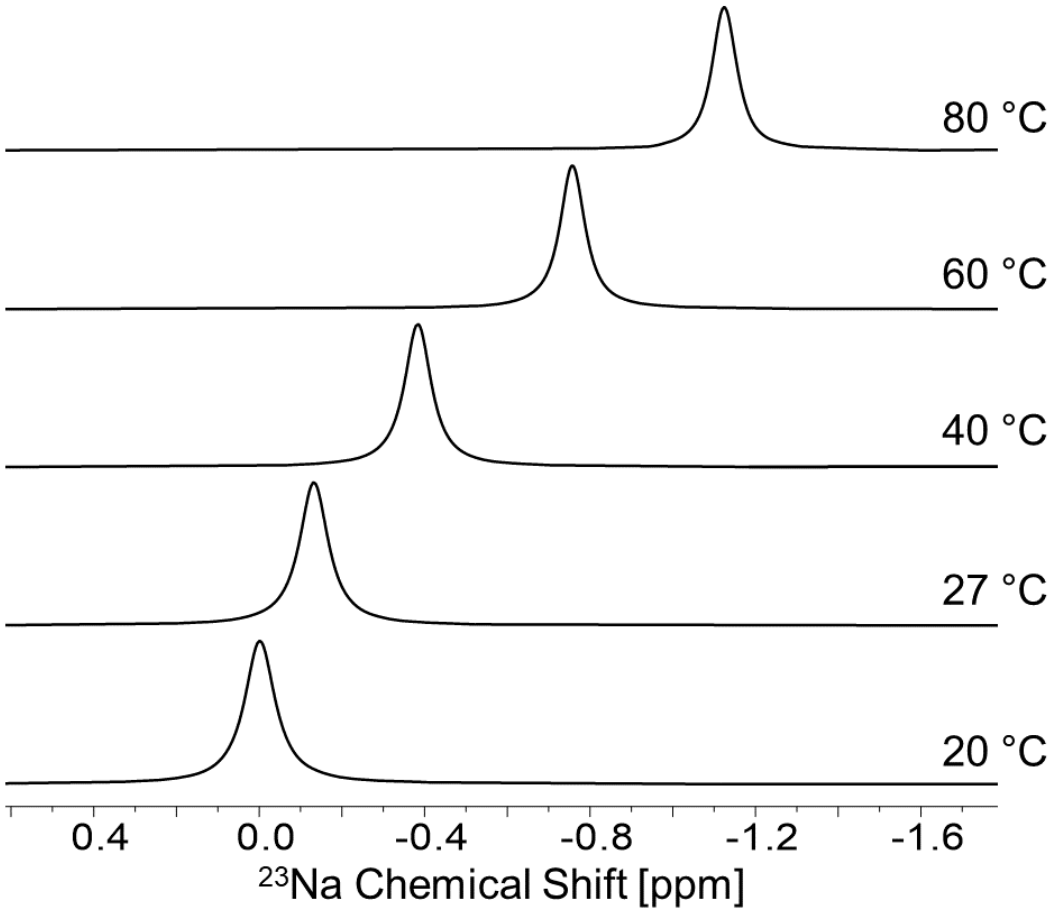

Figure S6. Single pulse, direct excitation ^{23}Na NMR spectra of 1 m $Na^{15}NO_2$ at temperatures ranging from 20 to 80 °C. At all temperatures, a single resonance is observed, which is attributable to a distribution of Na^+ ions in dynamic equilibrium that is fast relative to the NMR time scale. The spectra are normalized to the height of the resonance at each temperature. The chemical shift is referenced to the chemical shift of 1 m $Na^{15}NO_2$ at 20 °C.

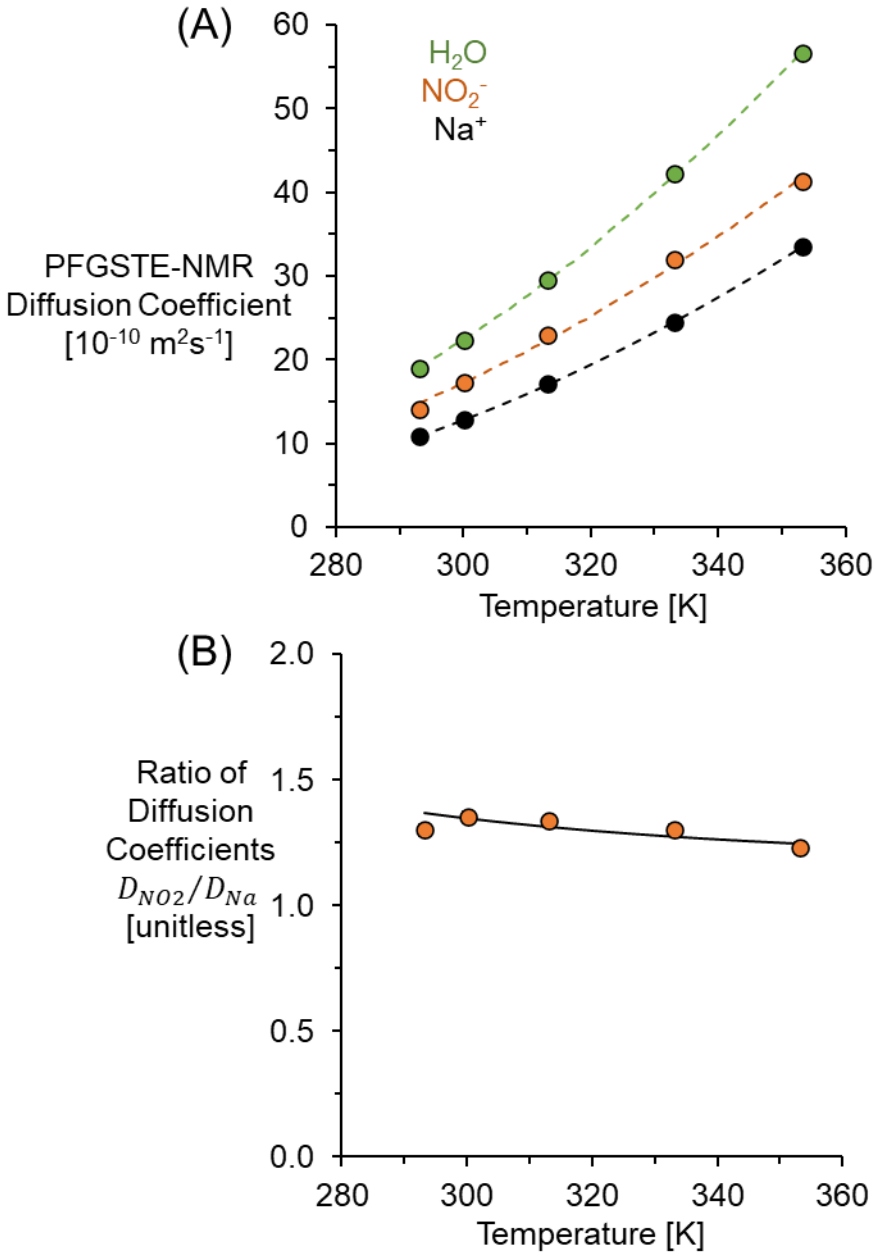

Figure S7. (A) Variable temperature PFGSTE-NMR data of 1 m $Na^{15}NO_2$ in H_2O. The data were fit by the VTF model. See page S8 for the fit parameters. (B) The ratio of nitrite and sodium diffusion coefficients.

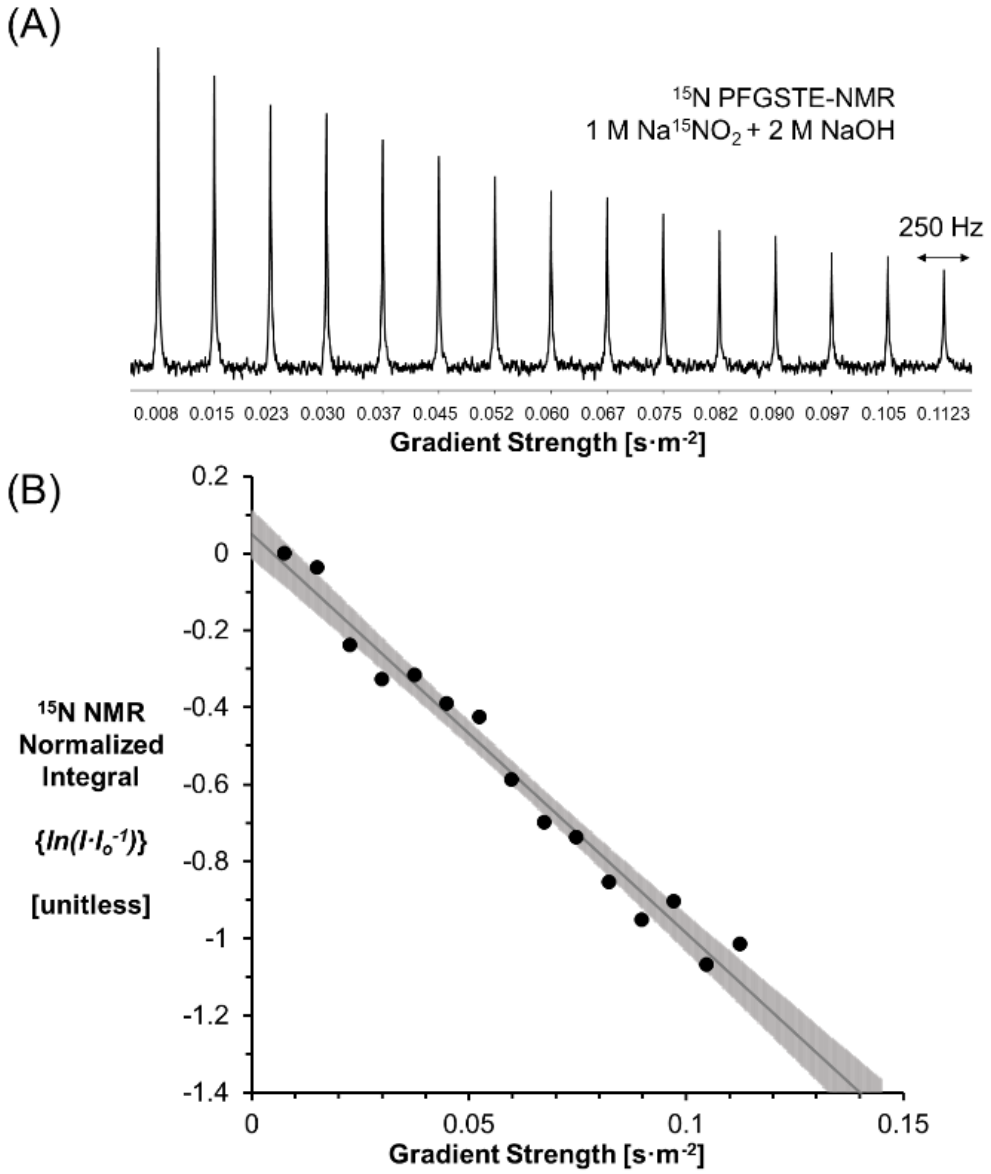

Figure S8. (A) ^{15}N PFGSTE-NMR spectra at 20 °C of aqueous solutions of 1 M Na^{15}NO$_2$ and 2 M NaOH representative of simplified compositions of nuclear waste. (B) Corresponding Stejskal-Tanner plot. Note the unit of concentration is moles/L.

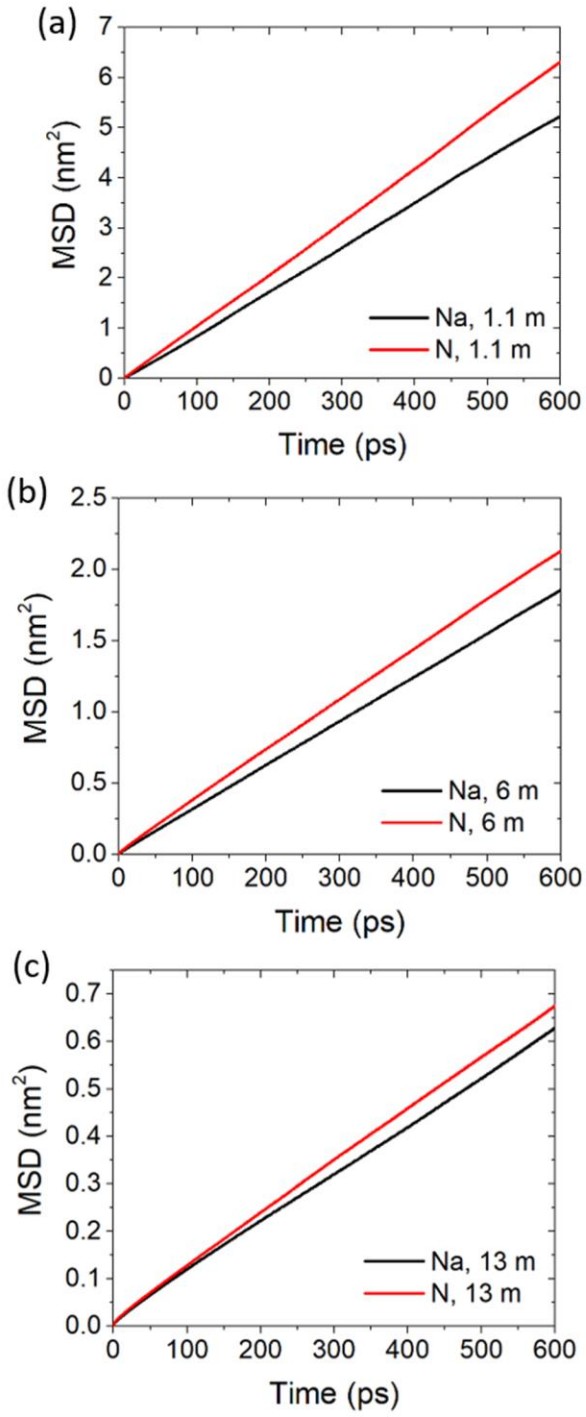

Figure S9. The mean square displacement of Na and N species in (a) 1.1 m, (b) 6 m and (c) 13 m $NaNO_2$ aqueous solutions from classical molecular dynamics simulation

WORKS CITED

1. D. S. Raiford, C. L. Fisk and E. D. Becker, *Anal Chem*, 1979, **51**, 2050-2051.
2. D. Van der Spoel, E. Lindahl, B. Hess, G. Groenhof, A. E. Mark and H. J. C. Berendsen, *J Comput Chem*, 2005, **26**, 1701-1718.
3. S. Nose, *Mol Phys*, 1984, **52**, 255-268.
4. W. G. Hoover, *Phys Rev A*, 1985, **31**, 1695-1697.
5. M. Parrinello and A. Rahman, *J Appl Phys*, 1981, **52**, 7182-7190.
6. T. Darden, D. York and L. Pedersen, *J Chem Phys*, 1993, **98**, 10089-10092.
7. H. J. Berendsen, J. P. Postma, W. F. v. Gunsteren and J. Hermans, Israel, 1981.
8. R. M. Cordeiro, M. Yusupov, J. Razzokov and A. Bogaerts, *The Journal of Physical Chemistry B*, 2020, **124**, 1082-1089.
9. B. Hess, H. Bekker, H. J. C. Berendsen and J. G. E. M. Fraaije, *J Comput Chem*, 1997, **18**, 1463-1472.
10. M. Hudelson, B. L. Mooney and A. E. Clark, *J Math Chem*, 2012, **50**, 2342-2350.
11. A. Macchioni, G. Ciancaleoni, C. Zuccaccia and D. Zuccaccia, *Chem Soc Rev*, 2008, **37**, 479-489.
12. T. R. Graham, D. J. Pope, Y. Ghadar, S. Clark, A. Clark and S. R. Saunders, *J Phys Chem B*, 2019, **123**, 5316-5323.
13. J. C. Mauro, Y. Z. Yue, A. J. Ellison, P. K. Gupta and D. C. Allan, *P Natl Acad Sci USA*, 2009, **106**, 19780-19784.